Divalent Transition Metals Substituted LaFeO$_3$ Perovskite Catalyst for Nitrous Oxide Decomposition

Asma H.A. Medkhali[1], Katabathini Narasimharao[1], Sulaiman N. Basahel[1] and Mohamed Mokhtar[1,2,*]

[1]*Chemistry Department, Faculty of Science, King Abdulaziz University, 21589 Jeddah, P.O. Box 80203, Saudi Arabia*

[2]*Physical Chemistry Department, National Research centre, El Buhouth St., Dokki, Cairo, Egypt*

Abstract: Divalent transition metals substituted LaFeO$_3$ type perovskite catalysts (LaFe$_{0.95}$M$_{0.05}$O$_3$ with M= Cu^{2+} and Ni^{2+}) were synthesized by hydrothermal method and characterized by using X-ray diffraction (XRD), temperature programmed reduction with H$_2$ (H$_2$-TPR) and N$_2$-physisorption techniques. The catalytic activity of the catalysts was tested for N$_2$O decomposition reaction. Enhancement in the catalytic activity was observed after substitution of Cu and Ni metal ions into LaFeO$_3$ framework. LaFe$_{0.95}$Ni$_{0.05}$O$_3$ showed higher catalytic activity than LaFeO$_3$ and LaFe$_{0.95}$Cu$_{0.05}$O$_3$ catalysts. The plausible reason for the increased activity is that LaFe$_{0.95}$Ni$_{0.05}$O$_3$ sample possessed high oxygen mobility than the other two samples.

Keywords: Perovskite, N$_2$O decomposition, Ni and Cu metal ions, XRD, H$_2$-TPR.

1. INTRODUCTION

Mixed conducting oxygen permeable (O-MIEC) materials are gaining significant attention for catalytic reactors, gas purification [1-3], natural gas conversion, coal gasification [4], and other selective oxidation of hydrocarbons [5-6]. The catalyst with perovskite structure ABO$_3$ attracts interest of the scientists due to high stability and catalytic properties. The unit cell in perovskite-type oxides consisting of B small cation which is catalytically active (usually transition metals) is in a six-fold coordination and the A (catalytically active) larger cation (usually rare earth, alkali, alkaline earth metals) is in a twelve fold coordination with the oxygen-anions [7]. Many required properties can be modified, including the unusual valence state of transition metal ions, the binding energy and diffusion of O in the lattice, the distance between active sites, and the magnetic and conductive properties of the these materials [8-11]. This modification made by the substitutions in A- and/or B-sites to control the structural defects. The modification in the catalytic properties of perovskites, by the insertion of dopants, remains the more intriguing to understand and study the catalytic processes on this material [12].

It was reported that LaFeO$_3$ is chemically stable in both reducing as well as oxidizing atmosphere [13]. The doped LaFeO$_3$ shows high electrical conductivity, outstanding thermal stability, high dielectric constant, low dielectric loss, moderate permittivity, susceptibility, polarizability, ferroelectricity, piezoelectricity therefore used as separator material in solid oxide fuel cells [14]. Doped LaFeO$_3$ also shows oxygen ion conductivity and has been studied for its applications in oxygen permeable membranes [15-17].

Nitrous oxide is one of causes the ozone depletion as well as of the greenhouse gases that cause the greenhouse effect. The global warming potential of N$_2$O (144) is found to be much higher than that of carbon dioxide gas (1). Therefore, the focus to control emissions this gas from the human sources was increased [18]. To control the N$_2$O emissions from industry and transportation sources there are different methods but the direct catalytic decomposition of N$_2$O is an attractive and economical option to control N$_2$O emission [19]. Recently, attention towards perovskite as active catalyst for N$_2$O decomposition was reported [19-23]. The stoichiometry and non-stoichiometry of LaCo$_{1-y}$O$_3$ and La$_{1-x}$CoO$_3$ perovskites on the catalytic activity of N$_2$O decomposition reaction were extensively studied [20]. The effect of partial substitutions on the B-site as in EuCo$_{1-x}$Fe$_x$O$_3$ [16], La$_{0.8}$Sr$_{0.2}$MO$_{3-\delta}$ (M = Cr, Fe, Mn, Co or Y) [22] and LaCo$_{1-x}$Fe$_x$O$_3$ (x= 0,0.2, 0.4, 0.6, 0.8) [17] as well as partial substitutions on the A-site as in Pr$_{1-x}$Ba$_x$MnO$_3$ (x = 0, 0.1–0.4) [23] were reported. It was also reported that the transition metal substituted catalysts offer relatively higher conversions in NO decomposition compared by the un-substituted catalyst [24]. In the present work, we are reporting the impact of the substitution of divalent transition metal cations (Cu^{2+} and Ni^{2+}) on LaFeO$_3$ structure and in N$_2$O decomposition activity.

*Address correspondence to this author at the Chemistry Department, Faculty of Science, King Abdulaziz University, 21589 Jeddah, P.O. Box 80203, Saudi Arabia; Tel: +966-500558045; Fax: +966-2-6952292;
E-mail: mmokhtar2000@yahoo.com, mmoustafa@kau.edu.sa

2. EXPERIMENTAL

2.1. Materials

Lanthanum nitrate $La(NO_3)_3.6H_2O$, iron nitrate $Fe(NO_3)_3.9H_2O$, Nickel nitrate $Ni(NO_3)_2.6H_2O$, Copper nitrate $Cu(NO_3)_2.3H_2O$ and Potassium hydroxide were purchased from Aldrich, UK and used as received.

2.2. Catalyst Synthesis

In a typical synthesis, stoichiometric amounts of lanthanum nitrate (0.025 mol) with other metals precursors dissolved in (100-150 mL) of deionized water, and 0.35 mol KOH solid powder were then added. After 1 h of ultrasonic stirring, the solution was transferred to a Teflon-lined autoclave (~75 vol.%) for hydrothermal treatment at 523 ^{o}K for 2 days. The so-obtained solid product was washed with DI water and dried overnight in an oven and homogenized by grinding and it was further calcined at 973 ^{o}K for 12 h in a muffle furnace.

2.3. Catalyst Characterization

XRD studies were carried out using a Bruker diffractometer (Bruker D8 advance target). The diffractograms were obtained using $CuK\alpha_1$ and a monochromator (λ = 1.5405Å) at 40 kV and 40 mA. H_2-temperature programmed reduction experiments were performed using Micromeritics AutoChem 2910 instrument. Calculated amount of catalyst initially treated with 10 %O_2-Ar at 573 ^{o}K for 30 min, and then the sample was purged with Ar gas. The sample temperature brought down to room temperature (298 K) by passing the air into the furnace. Then, the flow of the gas changed to 5 % H_2-Ar and the sample temperature increased to 837 ^{o}K at the rate of 5 ^{o}K/min. H_2-TPR patterns obtained by recording the TCD signal with respect to the time and temperature. The N_2 adsorpion-desorption isotherms were obtained from N_2-physisorption at 77 ^{o}K using Autosorb-1 (Quantachrome, USA). Out gassing of catalyst samples for 8 h at 423 ^{o}K was carried out prior to N_2-gas adsorption measurements.

2.4. N_2O Decomposition Measurements

The catalytic N_2O decomposition reaction was tested in a fixed-bed flow reactor. The amount of catalyst used is 500 mg in all the experiments. The temperature of the reaction was controlled by thermocouple that touched the catalyst bed zone. Prior to the catalytic test activation of the catalyst was performed by treating the catalyst under He flow at the reaction temperature. N_2O (1000 ppm) /He was passed with the aid of thermal mass flow controllers (He is a balance gas). The volume flow rate was fixed at 125cm^{3}min^{-1} (NTP) for all the investigated catalysts. The exit concentrations were monitored by non-dispersive infrared analyzer for the N_2O.

3. RESULTS AND DISCUSSION

3.1. Catalytic Decomposition of N_2O

N_2O conversion plot at different reaction temperatures on the lanthanum ferrite–based catalysts is presented in Figure **1**. The catalytic activity data indicated that the N_2O conversion over all the catalysts increases with increasing the reaction temperature from 637-823°K. The Ni and Cu substituted catalysts give relatively higher conversion compared to the un-substituted LaFeO₃ catalyst. The difference in the values of N_2O conversion was after 773°K, where the difference at 773°K was about 8% and at 823°K was about 20% for the Cu-substituted LaFeO₃.The Ni-substituted LaFeO₃ catalyst showed a difference of 11% at 773°K and it was about 28% at 823°K. The observed variation in the catalytic activity is due to the promotional effect of the substitution of divalent transition metals in LaFeO₃ perovskite catalysts. This effect may be attributed to the formation of the oxygen deficiency in the perovskite lattice.

The oxygen deficiency in this catalysts created by partial substitutions of Fe^{3+} by transition metal with different oxidation state (Cu^{2+} or Ni^{2+}). The oxygen deficiency causes oxygen mobility in the lattice at high
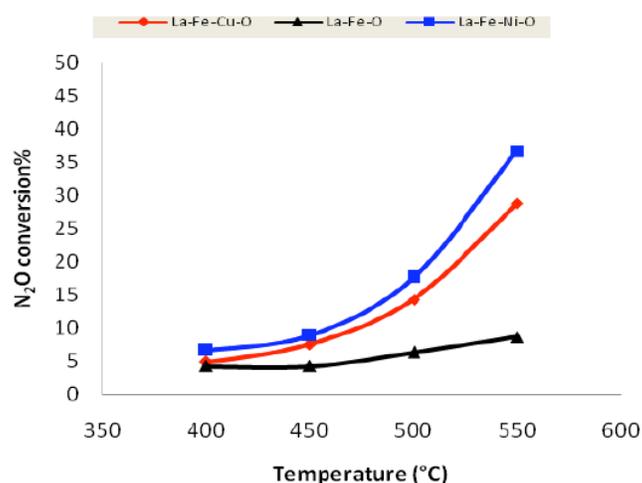
Figure 1: N_2O conversion % over LaFeO₃ and LaFe$_{0.95}$M$_{0.05}$O₃: 1000ppm N_2O, He as balance gas with flow rate 125 cm^3/min.

temperature (above $773^{o}K$) which generates the active sites for N_2O adsorption and then decomposition [10].
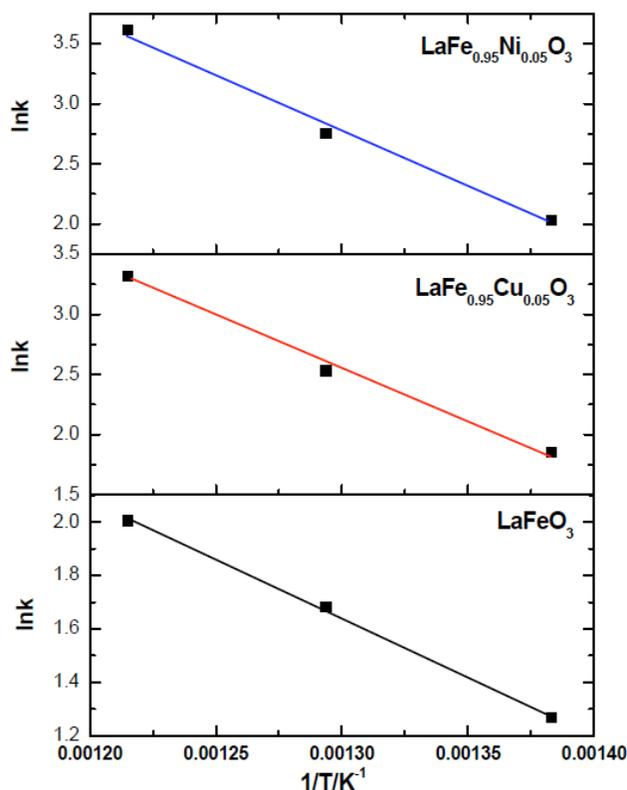
Figure 2: Arrhenius plots of activation energy of N_2O decomposition on the catalysts.

The determination of the activation energy (E_a) of N_2O decomposition over different substituted perovskite catalysts can throw more light on the role of divalent transition metal substitution in changing the mechanism of the catalyzed reaction. The apparent activation energy E_a was calculated using Arrhenius equation by determining the catalytic reaction rate constant (k) at different reaction temperatures. Figure **2** shows the Arrhenius plots of N_2O decomposition on different catalysts. The data obtained revealed the substitution of the Fe^{3+} by divalent cations is accompanied by an increase in the activation energy values. However, the catalytic activities of these catalysts were of higher than pure $LaFeO_3$. These results did not express the observed increase in the catalytic activity due to divalent cation substitution, simply because an increase and not a decrease in the value of E_a obtained upon divalent cation substitution in the $LaFeO_3$. This discrepancy has been solved by re-computing E_a values taking into consideration the possible changes in the values of the pre-exponential factor (A) in the Arrhenius equation [25-27]. In fact, the recalculation of E_a values adopting the A value of

$LaFeO_3$ catalyst to the other Cu^{2+} and Ni^{2+}-containing catalysts. The E_a^* values were obtained and given in the last column of Table **1** and these values are in decreasing trend upon divalent cation substitution to the $LaFeO_3$ catalyst. These findings show that substitution of Cu^{2+} and Ni^{2+} in $LaFeO_3$ perovskite did not modify the mechanism of NO decomposition, but brought an increase in the concentration of catalytically active constituents.

3.2. X-Ray Powder Diffraction

The XRD patterns for all the investigated solid catalysts are presented in Figure **3A** pure $LaFeO_3$ phase together with some unreacted La_2O_3 and Fe_2O_3 oxides were observed. Perovskite-like phase, with lower pattern intensity was observed after substitution of Cu^{2+} and Ni^{2+}cations in the $LaFeO_3$ perovskite framework. However, metal oxides such as CuO and NiO are not observed after the divalent cation substitution. The appearance of unreacted La_2O_3 and Fe_2O_3 phases after calcination at 973K for 12h indicate that higher temperature and/or longer time are necessary to complete the solid-solid interaction between La_2O_3 and Fe_2O_3 metal oxides to form pure single perovskite phase. However, the disappearance of NiO as well as CuO phases indicates the incorporation of these metal ions into the bulk of the perovskite structure. The incorporated metals (active phases) resulted in the pronounced increase in the catalytic activity of the divalent cation substituted perovskites catalysts.

3.3. H_2-Temperature Programmed Reduction (H_2-TPR)

In order to investigate the influence of the doping of divalent metals on the reducibility of $LaFeO_3$ sample, H_2-TPR experiments were used. Figure **4** shows H_2-TPR patterns of investigated samples. The TPR pattern of $LaFeO_3$ shows two stages reduction. In this case, the Fe^{3+} reduction started around 688 ^{o}K. Subsequently, a broad peak centered at $723^{o}K$ was obtained. Considering that the total experimental H_2 consumption is lower than the theoretical H_2 consumed for the total $Fe^{3+} \rightarrow Fe^{2+}$ reduction (0.789 *vs.* 2.06 mmol g^{-1}), the Fe^{3+} reduction below 1073 ^{o}K can be assigned to partial $Fe^{3+} \rightarrow Fe^{2+}$, and only 38.3 % of Fe^{3+} participated in this reduction step. For $LaFe_{0.95}Cu_{0.05}O_3$ sample, the reduction starting temperature shifted slightly to 637 ^{o}K, and two intense reduction peaks centered at 713 ^{o}K and 948 ^{o}K are observed.

Table 1:   Comparison of Activation Energies of the Catalysts

Catalyst	A	lnA	E_a(kJ/mole)	E_a^*(kJ/mole)[a]
$LaFeO_3$	7.34	1.99	36.47	36.47
$LaFe_{0.95}Cu_{0.05}O_3$	13.83	2.63	72.17	09.10
$LaFe_{0.95}Ni_{0.05}O_3$	14.96	2.71	77.95	11.13

[a]activation energy calculated at 823°K from Arrhenius equation using value of pre-exponential factor of $LaFeO_3$.
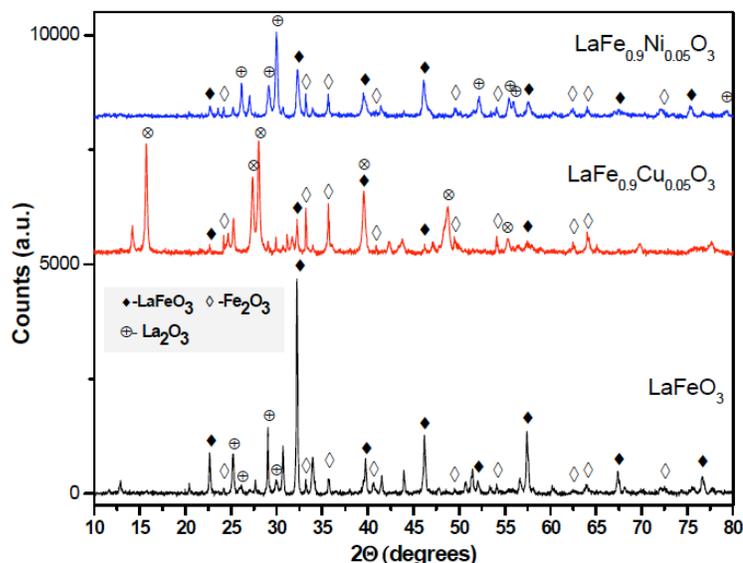
Figure 3: XRD patterns of perovskite catalysts.

A very similar pattern was observed in case of $LaFe_{0.95}Ni_{0.05}O_3$ sample. In comparison, a slight shift towards lower temperature was observed for the reduction peaks for metal incorporated samples. This shift can be explained by increase of oxygen vacancy concentration. It was reported that lower onset temperature of reduction peaks suggests that the material had better reducitbility and oxygen mobility. Therefore, $LaFe_{0.95}Ni_{0.05}O_3$ exhibited better activity than $LaFeO_3$ and $LaFe_{0.95}Ni_{0.05}O_3$.[28].

3.3. N₂ Adsorption/Desorption

Nitrogen adsorption-desorption isotherms at 77 K for $LaFeO_3$, Cu^{2+} and Ni^{2+} substituted $LaFeO_3$ perovskite samples are given in Figure **5**.

The isotherms of all the samples can be classified as type II in IUPAC classification with a type H3 hysteresis. The pore size distribution graphs are shown inset of Figure **5A** mesoporous and macroporous pore sizes were detected for $LaFeO_3$ pervoskite. However, the inclusion of Cu^{2+} ions in the structure (LaFeCu) resulted in a uniform mesoporous structure, while the

inclusion of Ni^{2+} ions substituted sample (LaFeNi) introduced extra micropores in addition to mesopores.

The specific surface area of the $LaFe_{0.95}Ni_{0.05}O_3$, determined by using BET equation and adsorption values from N₂ isotherms, was found to be ~14 m² g⁻¹, which is larger than that recorded for the $LaFeO_3$ (~10 m² g⁻¹). The addition of Ni^{2+} resulted in a slight
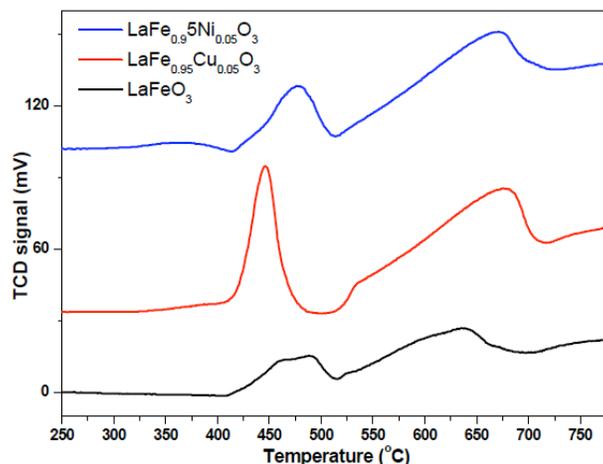
Figure 4: H₂-TPR patterns of investigated samples.
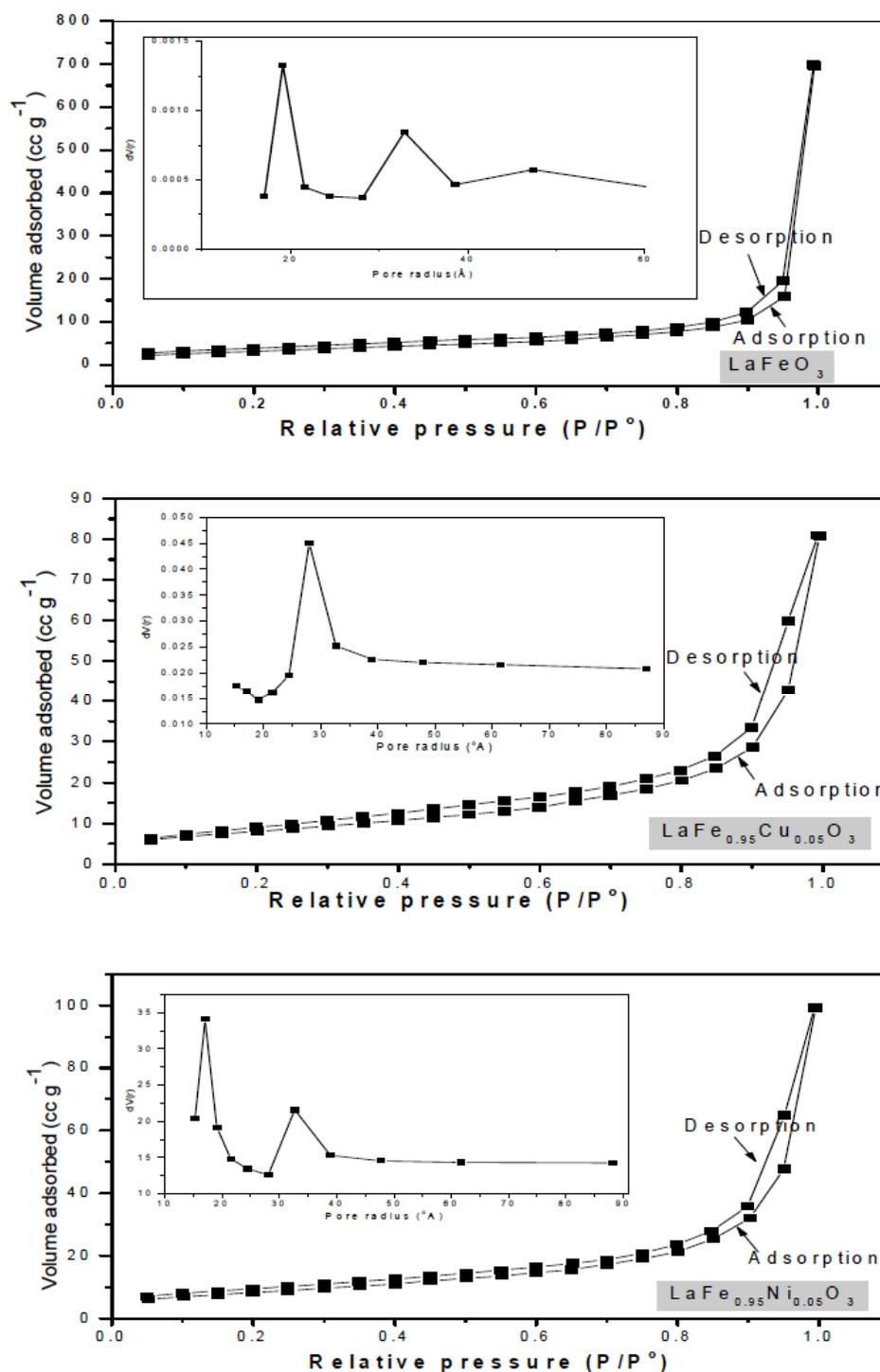
Figure 5: Nitrogen adsorption-desorption isotherms of the samples (inset pore size distribution patterns).

increase in surface area, whereas addition of Cu^{2+} did not show any significant change (~11 m^2 g^{-1}). The observed increase may be attributed to the creation of the extra micropore structure as well as oxygen vacancies upon Fe^{3+} substitution with Ni^{2+}.

The characterization results indicating that incorporation of Ni and Cu metal ions resulted in the

enhancement of oxygen mobility and slight increase of surface area, which could contribute to the catalytic activity [29].

CONCLUSION

The catalytic activity for N_2O decomposition reaction on the $LaFeO_3$ perovskite increased after substitution of

Fe^{3+} in B site of the perovskite by Cu^{2+} and Ni^{2+}. With increasing the reaction temperature, the catalytic activity was increased. The oxygen deficiency causes oxygen mobility in the lattice at high temperature (above 773 ^{o}K) seems to be higher for metal ion incorporated samples. The enhancement of oxygen mobility and slight increase of surface area resulted in the creation of more active sites for N_2O adsorption and then decomposition in case of Ni and Cu incorporated $LaFeO_3$ samples.

ACKNOWLEDGEMENT

REFERENCES

[1]   Meolin L, Ashok VJ, Yousheng S, Kevin K, Anil VV, inventors; Gas Res. Inst., assignee. Mixed ionic-electronic conductors for oxygen separation and electrocatalysis. United States patent US 5478444A. 1995 Dec.

[2]   Shao Z, Xiong G, Dong H, Yang W, Lin L. Synthesis, oxygen permeation study and membrane performance of a $Ba_{0.5}Sr_{0.5}Co_{0.8}Fe_{0.2}O_{3-\delta}$ oxygen-permeable dense ceramic reactor for partial oxidation of methane to syngas. Sep Purif Technol 2001; 25: 97-116.
http://dx.doi.org/10.1016/S1383-5866(01)00095-8

[3]   Balachandran U, Ma B. Mixed-conducting dense ceramic membranes for air separation and natural gas conversion. J Solid State Electrochem 2006; 10: 617-24.
http://dx.doi.org/10.1007/s10008-006-0126-y

[4]   Ikeguchi M, Mimura T, Sekine Y, Kikuchi E, Matsukata M, Reaction and oxygen permeation studies in $Sm_{0.4}Ba_{0.6}Fe_{0.8}Co_{0.2}O_{3-\delta}$ membrane reactor for partial oxidation of methane to syngas. Appl Catal A: Gen 2005; 290: 212-20.
http://dx.doi.org/10.1016/j.apcata.2005.05.033

[5]   Leo A, Liu S, Costa JC, Development of mixed conducting membranes for 69clean coal energy delivery. Int J Greenh Gas Control 2009; 3: -35767.

[6]   Zhu W, HanW, Xiong G, Yang W, Mixed reforming of simulated gasoline tohydrogen in a BSCFO membrane reactor. Catal Tod 2006; 118: 39-43.
http://dx.doi.org/10.1016/j.cattod.2005.11.088

[7]   Tejuca LG, Fierro JL, Eds. Structure and reactivity of perovskite-type oxides. Academic Press: Elsevier 1989.

[8]   Leontiou AA, Ladavos AK, Bakas TV, Vaimakis TC, Pomonis PJ, Reverse uptake of oxygen from $La_{1-x}Sr_x$ $(Fe^{3+}/Fe^{4+})O_{3\pm\delta}$ perovskite-type mixed oxides (x = 0.00, 0.15, 0.30, 0.40, 0.60, 0.70, 0.80, 0.90). Appl Catal A: Gen 2003; 241: 143-54.
http://dx.doi.org/10.1016/S0926-860X(02)00458-1

[9]   Tien-Thao N, Alamdari H, Zahedi-Niaki MH, Kaliaguine S, $LaCo_{1-x}Cu_xO_{3-\delta}$ perovskite catalysts for higher alcohol synthesis. Appl Catal A: Gen 2006; 311: 204-12.
http://dx.doi.org/10.1016/j.apcata.2006.06.029

[10]   Dhar GM, Srinivasan V, Surface oxygen bond energy, and kinetics and catalysis on perovskite oxide catalysts. Int J Chem Kinet 1982; 14: 435-38.
http://dx.doi.org/10.1002/kin.550140409

[11]   Voorhoeve RJH, Johnson DW, Remeika JP, Gallagher PK, Perovskite Oxides: Materials Science in Catalysis. Science 1977; 195(4281): 827-33.
http://dx.doi.org/10.1126/science.195.4281.827

[12]   Ivanov DV, Pinaeva LG, Isupova LA, Nadeev AN, Prosvirin IP, Dovlitova LS, Insights into the Reactivity of $La_{1-x}Sr_x$ MnO_3 (x = 0-0.7) in High Temperature N_2O Decomposition. Catal Lett 2011; 141: 322-31.
http://dx.doi.org/10.1007/s10562-010-0503-0

[13]   Climate Change-Emissions Overview -Nitrous Oxide. 13/9/2013 [cited 18/9/2013]; Available from: http://epa.gov/climatechange/ghgemissions/gases/n2o.html.

[14]   Kumar S, Vinu A, Subrt J, Bakardjieva S, Rayalu S, Teraoka Y, Labhsetwar N, Catalytic N_2O decomposition on $Pr_{0.8}Ba_{0.2}MnO_3$ type perovskite catalyst for industrial emission control. Catal Tod 2012; 198: 125-32.
http://dx.doi.org/10.1016/j.cattod.2012.06.015

[15]   Wu Y, Ni X, Beaurain A, Dujardin C, Granger P, Stoichiometric and non-stoichiometric perovskite-based catalysts: Consequences on surface properties and on catalytic performances in the decomposition of N_2O from nitric acid plants. Appl Catal B: Environ 2012; 125: 149-57.
http://dx.doi.org/10.1016/j.apcatb.2012.05.033

[16]   Wu Y, Dujardin C, Granger P, Tiseanu C, Sandu S, Kuncser V, Parvulescu VI, Spectroscopic Investigation of Iron Substitution in $EuCoO_3$: Related Impact on the Catalytic Properties in the High-Temperature N_2O Decomposition. J Phys Chem C 2013; 117: 13989-99.
http://dx.doi.org/10.1021/jp402211c

[17]   Gunasekaran N, Rajadurai S, Carberry JJ, Catalytic decomposition of nitrous oxide over perovskite type solid oxide solutions and supported noble metal catalysts. Catal Lett 1995; 35: 373-82.
http://dx.doi.org/10.1007/BF00807194

[18]   Wu Y, Cordier C, Berrier E, Nuns N, Dujardin C, Granger P, Surface reconstructions of $LaCo_{1-x}Fe_xO_3$ at high temperature during N_2O decomposition in realistic exhaust gas composition: Impact on the catalytic properties. Appl Catal B: Environ 2013; 140-141: 151-63.
http://dx.doi.org/10.1016/j.apcatb.2013.04.002

[19]   Hammou A, Guindet J, Eds. The CRC Handbook of Solid State Electrochemistry (Gellings PJ, Bouwmeester HJM), CRC Press Inc: 1997.

[20]   Steele BCH, Heinzel A, Materials for fuel-cell technologies. Nature 2001; 414: 345-52.
http://dx.doi.org/10.1038/35104620

[21]   Chao SJ, Song KS, Ryu IS, Seo YS, Rayoo MW, Kang SK, Characteristics of methane combustion over La–Cr–O catalysts. Catal Lett 1999; 58: 63-6.
http://dx.doi.org/10.1023/A:1019092809562

[22]   Minh NQ, Ceramic fuel cells. J Amer Ceram Soc 1993; 76: 563-88.
http://dx.doi.org/10.1111/j.1151-2916.1993.tb03645.x

[23]   Steele BCH, Oxygen ion conductors and their technological applications. Mater Sci Eng B 1992; 13: 79-87.
http://dx.doi.org/10.1016/0921-5107(92)90146-Z

[24]   Tofan C, Klvana D, Kirchnerova J, Direct decomposition of nitric oxide over perovskite-type catalysts: Part I. Activity when no oxygen is added to the feed Appl Catal A: Gen, 2002; 223: 275-86.
http://dx.doi.org/10.1016/S0926-860X(01)00764-5

[25]   Radwan NRE, Mokhtar M, El-Shobaky GA, Surface and catalytic properties of CuO and Co_3O_4 solids as influenced by treatment with Co^{2+} and Cu^{2+} species. Appl Catal A: Gen 2003; 241: 77-90.
http://dx.doi.org/10.1016/S0926-860X(02)00459-3

[26]   El-Shobaky HG, Mokhtar MM, Effect of Li_2O and CoO-doping of CuO/Fe_2O_3 system on its surface and catalytic properties. Appl Sur Sci 2007; 253(24): 9407-13.
http://dx.doi.org/10.1016/j.apsusc.2007.06.001

[27]   He F, Zhao K, Huang Z, Li Xa, Wei G, Li H, Synthesis of three-dimensionally ordered macroporous $LaFeO_3$ perovskites and their performance for chemical-looping reforming of methane. Chin J Catal 2013; 34(6): 1242-49.
http://dx.doi.org/10.1016/S1872-2067(12)60563-4

[28]   Huheey JE, Keiter EA, Keiter RJ, Chemistry. Principles of structure and reactivity. Harper Collins: College Publishers, 1993.